Statistical model for the prediction of lung deformation during video-assisted thoracoscopic surgery

Valentin Boussot, Jean-Louis Dillenseger

Statistical model for the prediction of lung deformation during video-assisted thoracoscopic surgery

Valentin Boussot[a] and Jean-Louis Dillenseger[a]

[a]INSERM, U1099, Rennes, France; Université de Rennes 1, LTSI, Rennes, France

ABSTRACT

Accurate lung nodule localization during video-assisted thoracic surgery (VATS) for the treatment of early stage lung cancer is a surgical challenge. Recently, a new minimally invasive approach for nodule localization during VATS has been proposed, which consists in compensating by a biomechanical model the very large lung deformations occurring before and during surgery. This estimation of the deformations allows to transfer the position of the nodule visible on the preoperative CT to an acquisition of the lung performed during the operation using a Cone-Beam CT scanner (CBCT_2). But, in this approach, an additional CBCT acquisition (CBCT_1) must also be acquired just after the patient is placed in the operative position in order to estimate the deformations due to the change of the patient's position, from supine during the CT acquisition to lateral decubitus in the operating room. Our goal is to simplify this procedure and thus reduce the radiation dose to the patient. To this end, we propose to improve this solution by replacing the CBCT_1 acquisition by a model allowing to predict these deformations. This model is defined using the lung state information from CBCT_2 and a general statistical motion model built from the position change deformations already observed on other patients. We have data from 17 patients. The method is evaluated with a leave-one-out cross-validation on its ability to reproduce the observed deformations. The method reduces the average prediction error from 12.14 mm without prediction to 8.12 mm for an average prediction, and finally to 6.33 mm for a prediction with our model fitted to CBCT_2 only.

Keywords: General statistical motion model, Images Registration, CBCT, Lung deformation, Video-assisted thoracic surgery (VATS)

1. INTRODUCTION

Lung cancer is the leading cause of cancer death in the world for both men and women. Its mortality rate depends largely on the stage at which it is diagnosed. In the case of early detection, *i.e.* when cancer cells are still confined to the tissue of origin, the reference treatment is video-assisted thoracic surgery (VATS). The operation consists of removing the small area of the lung that contains the lesion under video guidance in a procedure called Wedge. To perform this procedure, the surgeon makes 3 incisions of about 3 cm in diameter in the chest, one for the endoscope and two to introduce the instruments. This minimally invasive operation allows a better and faster recovery and gives the patient a good chance of survival.

The localization of the pulmonary nodule during this operation is a prerequisite for its successful completion. However, the precise localization of the nodule to within 5 mm presents a difficulty from a surgical point of view. Indeed, the nodule is not visible from the surface of the lung and the small incisions to access the lung do not allow the surgeon to palpate it. The nodule is however visible on the preoperative CT, but there is a great anatomical disparity between the preoperative and intraoperative configurations, due to the large pulmonary deformations introduced during surgery. These deformations are of two kinds. On the one hand, the patient is in dorsal decubitus position during the CT, but he is placed in lateral decubitus on the operating table. On the other hand, the incisions made by the surgeon allow air to enter the pleuropulmonary space which produces a strong collapse of the lung into the mediastinum called pneumothorax. These deformations greatly modify the shape and internal pulmonary structures and thus the position of the nodule in relation to the reference CT.

Further author information: (Send correspondence to V. Boussot)
V. Boussot: E-mail: valentin.boussot@univ-rennes1.fr
J-L. Dillenseger: E-mail: jean-louis.dillenseger@univ-rennes1.fr

In current practice, localization is based on the introduction of a marking device (needles, hook wires, microcoils or dyes) into the lung during an initial preoperative percutaneous procedure under fluoroscopic and CT guidance. However, this invasive percutaneous preoperative procedure leads to high complication rates. In order to avoid this preoperative procedure, Rouzé *et al* proposed a totally non-invasive localization approach based on intraoperative imaging only.[1] A Cone-Beam CT scan (CBCT_2) is performed during the operation. This acquisition allows first to identify and localize the nodule in the CBCT, and then to guide the surgeon to this nodule. However, this solution suffers from a problem of reliability in the case of low density or deep nodules. Indeed, on the one hand, the quality of the CBCT image is reduced compared to a CT image with a lower contrast between the nodule and the surrounding lung parenchyma and on the other hand, pneumothorax leads to atelectasis, *i.e.* a high densification of the lung tissue. These two problems make the segmentation of these types of nodule impossible. To overcome this problem, Alvarez *et al* proposed to model the deformations of the lung by a biomechanical model to transfer the position of the nodule visible in CT on the CBCT_2.[2] As the deformations of the lung are very large and of different origins, Alvarez *et al* in their approach decided to acquire an intermediate CBCT volume (CBCT_1) just after the patient is placed in the operative position but before the pneumothorax. This CBCT_1 allows: 1) to estimate the deformations due to the change in the patient's position by a registration between the preoperative CT and the CBCT_1 and 2) to establish the initial position of the biomechanical model in order to simulate the deflation (pneumothorax) of the lung towards the surfaces seen on the CBCT_2. This estimation is essential for a good simulation of the pneumothorax and its allows to compensate initially for non-rigid deformations of the order of 1 cm on average and up to 30 mm for some clinical cases.

The objective of our work is to simplify this protocol and to reduce the radiation dose per patient by eliminating the intermediate CBCT_1 acquisition. To do so, instead of this acquisition, we will try to predict the deformations due to the change of the patient's position from the CT and CBCT_2 alone. This prediction will be based on a statistical model of movements established from the deformations already observed on the data of the previous patients who had the 3 acquisitions (CT, CBCT_1 and CBCT_2).

2. MATERIALS AND METHODS

2.1 Data

We have data from 17 patients, 12 patients included for a wedge nodule resection performed on the right lung and 5 patients for a nodule present in the left lung. The VATS surgical intervention was performed at the Rennes University Hospital, Rennes, France. This study was approved by the local ethics committee and the patients gave their informed consent prior to the procedure.

For each patient we have three volumes: 1) a preoperative CT, where the patient is in the supine position and was instructed to hold his breath during the capture (end of inspiration cycle); 2) a CBCT acquisition, called CBCT_1, performed during the operative phase, *i.e.* the patient is in lateral decubitus under sedation and mechanical ventilation. However, this acquisition is performed before the incisions therefore the lung is completely inflated; and 3) a CBCT acquisition, called CBCT_2, made after the thorax perforation with the resulting pneumothorax. Figure 1 shows an axial view of these 3 images.

We have built one deformation model for the right lung and one for the left lung. However, for the sake of clarity, in this paper we will present and evaluate only the deformation model for the right lung. The construction of the model for the left lung followed the same methodological approach.

2.2 Method workflow

The global workflow of the study is presented Figure 2.

In the learning phase, we had at our disposal the CT-CBCT_1 image pair for each patient. For our protocol we need the lung lobes segmented in CT and the spine segmented in CBCT modality. The idea is: a) for a given patient, to estimate the deformation field of the change of pose between CT and CBCT_1. For this purpose, CBCT_1 is aligned to the CT by a rigid spine registration. Then, the deformation $T(.)$ of the lung due to the change of pose is estimated by elastic registration between CT and CBCT_1; b) to establish a matching field between the lungs of the several patients. For this, we align the CT of the different patients to a model lung.

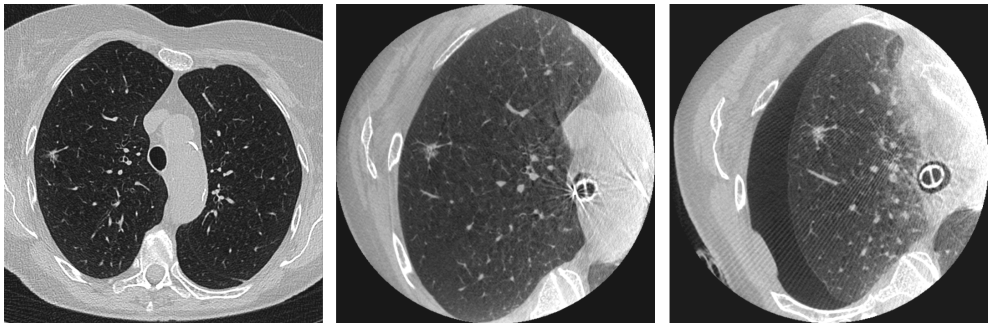

Figure 1. Slices in approximately the same transversal plane of, from left to right, the preoperative CT (supine position); the intraoperative CBCT_1 (lateral decubitus position) and intraoperative CBCT_2 with the pneumothorax

This is done by inter-patient registration of the segmented lungs in the CT. This matching field $T_{i,t}(.)$ between each patient's lung and the model lung ensures that each sampled vector accounts for the deformation of the same lung region regardless of the patient; c) create a model of lung tissue deformations using a weighting PCA computed on a parsimonious sample x_j of the different deformation fields describing the pose change. This allows us to create a deformation model with degrees of freedom corresponding to the main deformation modes observed.

In the prediction phase for a new patient, we have at our disposal the preoperative CT and the CBCT_2 after pneumothorax. Our starting assumption is that the pleuropulmonary space does not undergo deformation between CBCT_1 and CBCT_2 but undergoes significant deformation by the change in patient position. The segmented pleuropulmonary space on CBCT_2 thus gives the shape of the lung surface after deformations due to the change of pose. The prediction of the change of pose deformation can be formulated as an inverse problem. For this purpose: a) CBCT_2 is aligned to CT by rigid spine registration; b) CT is aligned to the model lung by inter-patient registration; c) the principal deformation modes are identified by an inverse problem from the lung surface in CT and the pleuropulmonary space surface in CBCT_2; d) once the principal modes are identified, the model vectors are associated with a deformation field by a third order B-Spline interpolation.

The key points of our method (segmentation, registration, creation of the statistical model of deformations and resolution of the inverse problem) will now be detailed.

2.3 Segmentations

In our method we need to segment 3 anatomical structures: 1) the 3 lobes of the right lung or the 2 lobes of the left lung in the CT modality, 2) the spine on the CBCT_1 and CBCT_2 images and 3) the pleuropulmonary space visible in the CBCT_2.

1) The anatomical description of the lobes was performed with the open source tool Chest Imaging Platform (CIP) present on the 3D Slicer software.[3] It is a semi-automatic tool that segments the 5 lobes of both lungs. This algorithm must be manually initialized with a set of markers to help identify the lobe boundaries.

2) In our case, a coarse segmentation of the spine is sufficient, it is performed by an automatic algorithm based on the intensities with a priori on the position of the spine that depends on the lung that is operated.

3) The description of the pleuropulmonary space in CBCT_2 is the union of the deflated lung and the air present in the pleural space. This description was achieved by an iterative region growing approach implemented by the 3D slicer software. The implemented algorithm requires manual initialization and some interactive post-processing.

2.4 Large deformation image registration method

In our method, two steps require the estimation of a large deformation field between two images: the estimation of the deformation fields between CT-CBCT_1 for one patient and the inter-patient alignment of the CTs. To solve them we used the classical multiresolution iterative registration method based on image intensity implemented in Elastix.[4] In both cases, the similarity measures measured between the fixed image I_f and the moving image I_m

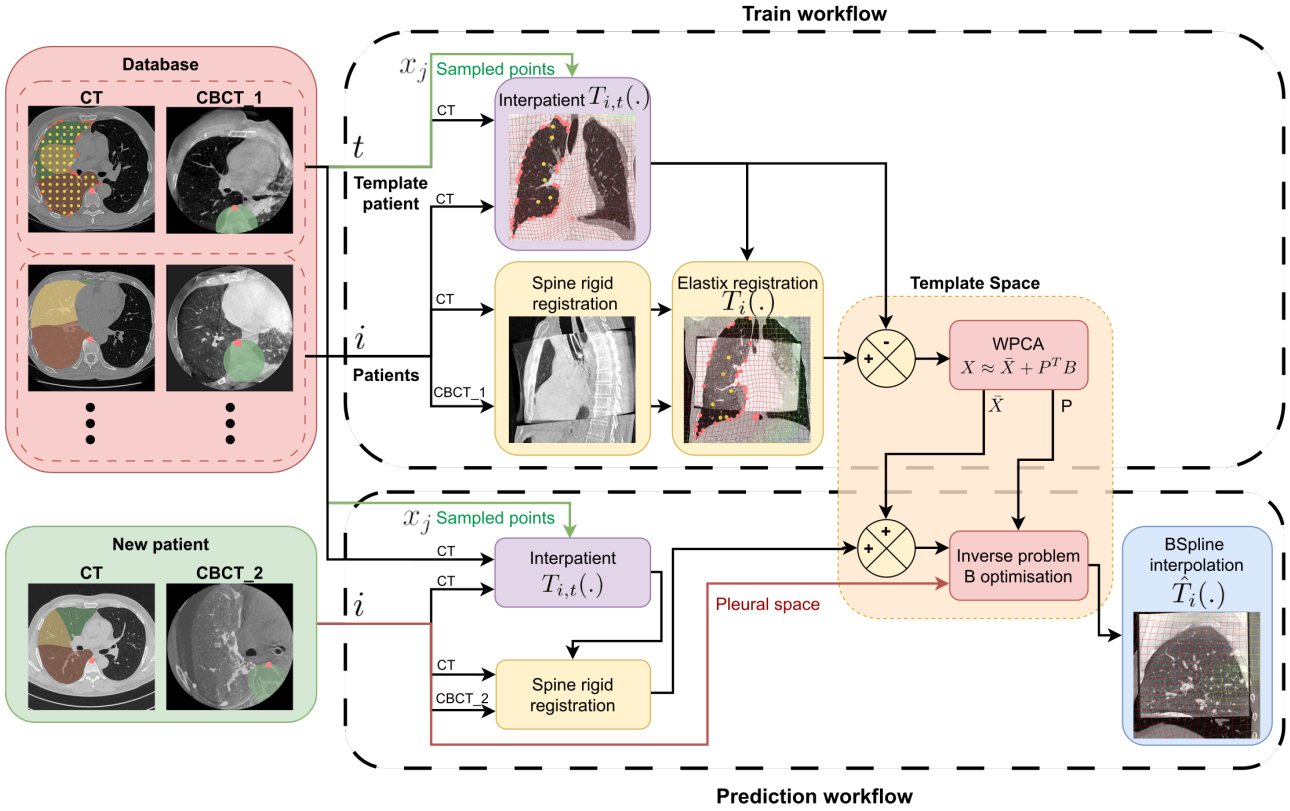

Figure 2. Workflow of our study

are estimated from N random samples within the intersection of fixed image Ω_f and the domain of the moving image Ω_m. They have been optimized with an adaptive stochastic gradient optimizer. Four image resolutions were required to allow the algorithm to account for large displacements and avoid local minima. The final deformation $T_\mu(x)$ (see Equation 1) uses a 3rd order B-Splines $\beta^3(.)$ deformation model with control points x_k arranged on a homogeneous grid with $\sigma = 20$ mm spacing on the highest resolution in the fixed image domain Ω_f.

$$T_\mu(x) = x + \sum_{x_k \in \Omega_f} p_k \beta^3\left(\frac{x - x_k}{\sigma}\right) \qquad \mu = \{p_{1x}, p_{1y}, p_{1z}, ..., p_{Nx}, p_{Ny}, p_{Ny}\} \tag{1}$$

2.4.1 CT-CBCT_1 registration

The estimation of the deformations due to the change of patient's pose is performed by an elastic registration of the CT-CBCT_1 image pair. This estimation is done in 2 steps, 1) a rigid registration and 2) an elastic registration.

1) The rigid registration aims at aligning the structures not affected by the deformations in order to estimate in a second time the mean deformation and the main deformation modes with deformation fields relative to this fixed reference point. For this purpose, the two volumes are initially aligned to the spine. This is done by first applying a 90 degree transformation, and then the two volumes are aligned using two matched markers manually placed on one of the vertebrae in the CT and CBCT_1. A rigid registration is then performed using a normalized cross-correlation similarity measure estimated from 3000 samples on the spine in the CBCT.

2) One of the key points of the elastic registration is the cost function that estimates the displacement of control points between the fixed image I_f and the moving image I_m. In our case, we decided to integrate two similarity measures in our cost function: a normalized cross-correlation (NCC) on the amplitudes of the image

gradients as originally proposed by Haber *et al*[5] and a normalized mutual information on the image intensities (MI):

$$C(\mu; I_f, I_m) = -NCC(\mu; ||\Delta I_f||_2, ||\Delta I_m||_2) - \alpha MI(\mu; I_f, I_m), \qquad \alpha = 1 \tag{2}$$

where $||\Delta I||_2$ denoting a magnitude operator on the gradient of the image I.

The two similarity measures are estimated from 1000 samples extracted within the CT lung volume. The few degrees of freedom of the deformation model allow to have a good description of the deformation by posing the problem well enough to avoid the need of regularization.

The choice of hyperparameters for these algorithms was found by an exhaustive search using a subset of patients (6 clinical cases) for whom markers matched on both images were placed by the pulmonary surgeon (≈ 30 for each case). We chose the combination that yielded the lowest Target Registration Error (TRE) between the markers. The median error was less than 1 mm, which is consistent with the resolution of the voxels in the images

2.4.2 Inter-patient lung matching

The matching field between each patient's lung and a model lung is achieved by the registration of each of the lobes of both lungs. The model lung was selected as the lung with the largest volume in the database. This choice is important because the displacement vectors will be sampled spatially in the model lung and a contraction the spacing of the sampled positions rather than a dilation is desirable.

The lungs between patients show large disparities in size and shape. The challenge of lung registration is not to match their fine structures to each other but to match anatomically close regions. To do this, an affine registration process first compensates for differences in size and orientation. A non-rigid registration is then applied to compensate for the difference in shape. As we want to perform a lobe registration without influence from the outside, as Wu *et al*[6] we assign a very low value (-2000) to the voxels outside the lobes. The similarity measure to be minimized is the combination of the cross-correlation (CC) and a penalty term P (bending energy) that penalizes sharp changes in local transformation curvature in order to make the deformations as smooth as possible while fitting the shape of the lung model. The cost function takes the following form:

$$C(\mu; I_f, I_m) = -CC(\mu; I_f, I_m) + \alpha P(\mu) \qquad \alpha = 10 \text{ and } P(\mu) = \frac{1}{N}\sum_{i}^{N} ||H_{(T_\mu(x_i))}||_F^2 \tag{3}$$

where $H_{(T_\mu(x))}$ is the Hessian matrix of the transformation $T_\mu(.)$.

2.5 Weighting principal component analysis

A PCA model was used to observe the main deformation modes of the lung population from its mean deformation.

To form our statistics, we used two types of sampling. On the one hand, a volume sampling using a grid of points in the model lung region with a spacing of 16 mm and which includes 866 points. This type of sampling aims to recover the initial deformation field with a B-Spline interpolation. On the other hand, a sampling of the lung surface of the model lung. These sampling points correspond to the nodes of a triangular mesh obtained by a smooth mesh of the model lung segmentation for a total of 7218 points. This type of sampling allows to associate a lung shape to the model.

For each patient i, the deformation field modeling the pose change is sampled using these points, which are previously matched to the patient's CT lung using the model lung matching field. Each sampled vector is flattened and concatenated into a vector $\vec{x_i} \in \mathbb{R}^{(866+7218)*3}$. The set of vectors in the training base thus formed is assembled into a matrix X with I rows (number of patients) and $J \times 3$ columns (Number of vectors $\times$ 3). Formally:

$$X_{i,j} = T(T_{i,t}(x_j)) - T_{i,t}(x_j) \tag{4}$$

One of our major problems is that CBCT field of view (FOV) is limited and does not allow to capture the whole lung. The estimation of its deformation is only valid in this FOV. In order not to bias the mean deformation and the main observed deformation modes, we defined a weight that quantifies for each patient and for each vector the confidence we have in the described estimation. The weights corresponding to the vector are functions of their arrival position x_j in the CBCT_1: in the inside of the FOV the weight is fixed at 1 and in the outside the weight decreases exponentially with respect to its distance to the CBCT FOV with a half-life fixed at a distance of $p = 10$ mm:

$$w^*_{i,j} = e^{\frac{\log(0.5)}{p} d_i^{fov}(x_j)} \qquad w_{i,j} = \frac{w^*_{i,j}}{\sum_{k=1}^{I} w^*_{k,j}} \tag{5}$$

where $d_i^{fov}(.)$ corresponds to a distance map from the FOV of the CBCT_1 after rigid registration of the CT/CBCT_1 for the patient i. It is obtained by a unsigned Danielson distance map[7] calculated from a cylindrical mask adjusted to CBCT_1 and resampled in the CT domain. The weight matrix W is normalized so that the columns are summed to 1.

Figure 3 shows the 2 kind of sample points (volume in yellow and surface in red) and the confidence map quantified by weights (color map).

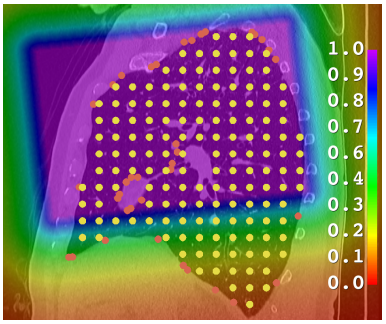

Figure 3. CT-model volume with the 2 types of sample points (volume in yellow and surface in red) and the confidence map. The confidence function is encoded by a color map, the purple region corresponds to the CBCT_1 field of view

The weighted average deformation is calculated as follows:

$$\mu_j = \sum_{i=1}^{I} w_{i,j} x_{i,j} \tag{6}$$

The construction of the deformation model poses the problem of the low rank approximation of the matrix X. Let be the following optimization problem:

$$\arg\min_{P,B} \chi^2 = \sum_{ij} w_{ij} [x_{i,j} - \mu_j - \sum_{k=1}^{M} p_{k,j} b_{k,i}]^2 \tag{7}$$

with $P = (p_{k,j})_{1 \leq k \leq M, 1 \leq j \leq J}$ a matrix whose column are the principal components to find, and $B = (b_{k,i})_{1 \leq k \leq M, 1 \leq i \leq I}$ is a matrix of coefficients to fit X using P. The mode number M, is assumed to be small and P is subject to an orthonormality constraint, $P^T P = \mathbb{1}$. To solve this optimization problem we used an implementation of an Expectation-Maximization type algorithm proposed by Bailey (EMPCA).[8]

2.6 Inverse problem formulation

The deformation modes for a new patient are searched so that the surface of the CT lung deformed by the model fits the pleuropulmonary space surface extracted from CBCT_2. For this purpose, the CBCT_2 is first aligned

on the CT using a rigid registration of the spine in order to remove the rigid components. The CT is also aligned to the lung model using the registration described in section 2.4.2.

The objective is then to estimate the deformation modes from the measurement of the distances between the mean deformation surface described by the lung model and the pleuropulmonary space surface of CBCT_2. For a quick measurement of these distances, the surface nodes of the mean model are immersed in an square signed Danielson distance map[7] calculated from the pleuropulmonary space mask resampled in the CT volume domain (see Figure 4).

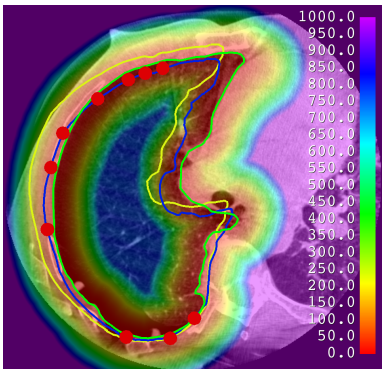

Figure 4. Superimposed on a slice of the CBCT_2 volume: in green the contour of the pleuropulmonary space in CBCT_2 with the distance map to this contour represented as a color map; in yellow the contour of the CT lung aligned on the CBCT_2; in blue the boundary of the mean deformation surface described by the lung model, the red markers are the surface nodes of the mesh projected in the distance map.

The main mode B is estimated by the following optimization problem:

$$\arg\min_{B} L_i = \frac{1}{N} \sum_{j \in \Omega_j} \sqrt{d(\mu_j + P_j^T B)} \tag{8}$$

where $d(.)$ corresponds to a distance map from pleuropulmonary mask and $P_j^T \in \mathbb{R}^{3\times M}$ a principal component matrix of the j th vector from a subset of vectors localized at the lung surface in the FOV of CBCT_2. The points on the medial face and the diaphragm region are removed from the set.

To make the optimization method more robust to outliers, we applied a non-linear function that allows to give less importance to these points. To solve this optimization problem we applied adagrad:

$$B_{t+1} = B_t - \frac{\eta}{\sqrt{g_t g_t^T}} g_t \text{ with } B_0 = [0, 0, ...], \eta = 1 \text{ and } g_t = \frac{\partial L}{\partial B} = \frac{1}{N} \sum_i P_j \frac{d'(\mu_j + P_j^T B)}{2\sqrt{d(\mu_j + P_j^T B)}} \tag{9}$$

where $d'(x) = \frac{\partial d(x)}{\partial x}$ is the gradient image of the distance map.

3. EVALUATION

3.1 Evaluation protocol

The experiments were conducted in a leave-one-patient-out procedure on the 12 patients operated on the right lung. We propose a quantitative evaluation of our method. For a test patient, we predict, using our model, CT and CBCT 2, the pose change deformations. We then compare this prediction to the deformations estimated by the elastic registration of the CBCT_1 to the CT used for the learning as described in the workflow (section 2.2) and considered as reference truth. The criterion consists in measuring on the test data, the Target Registration Error (TRE) which is the L2-norm between the volume sampling points x_j projected by the estimated deformation $T(x_j)$ (reference truth) and by the predicted deformation $\hat{T}(x_j)$ within the FOV of CBCT_1:

$$TRE = ||T(x_j) - \hat{T}(x_j)||_2 \tag{10}$$

We compared the performance obtained by 4 prediction models: (*Rigid*) no prediction (rigid registration between CT and CBCT_2); (*Mean*) the prediction of the mean deformation of our model; (*Optimal*) the prediction with the estimation of the deformation modes by solving the inverse problem of our method on the pleuropulmonary surface of CBCT_1; and, (*Prediction*) the prediction with the estimation of the deformation modes by solving the inverse problem of our method on the pleuropulmonary surface visible in the CBCT_2.

The aim of the (*Optimal*) test was to verify the accuracy of the model using the same conditions (pleuropulmonary space) as during training. On the other hand, in clinical routine this prediction model cannot be used because we will no more have access to CBCT_1.

3.2 Results

Figure 5 and Figure 6 show the error distribution for all the 12 patients according to the 4 predictions. The average median error for each patient for each prediction is (*Rigid*) 12.79 mm, (*Mean*) 8.09 mm, (*Optimal*) 3.86 mm and (*Prediction*) 6.33 mm.

Figure 7 shows the modeling performance of our wPCA model on the test data as a function of the number of M modes used to fit the training data (see (7)). The performance of the 12 models is estimated in the form of the characteristic values of the distribution of errors on the 12 test patients: median value (50%), first and third quartiles (25% and 75%) and limits (5% and 95%).

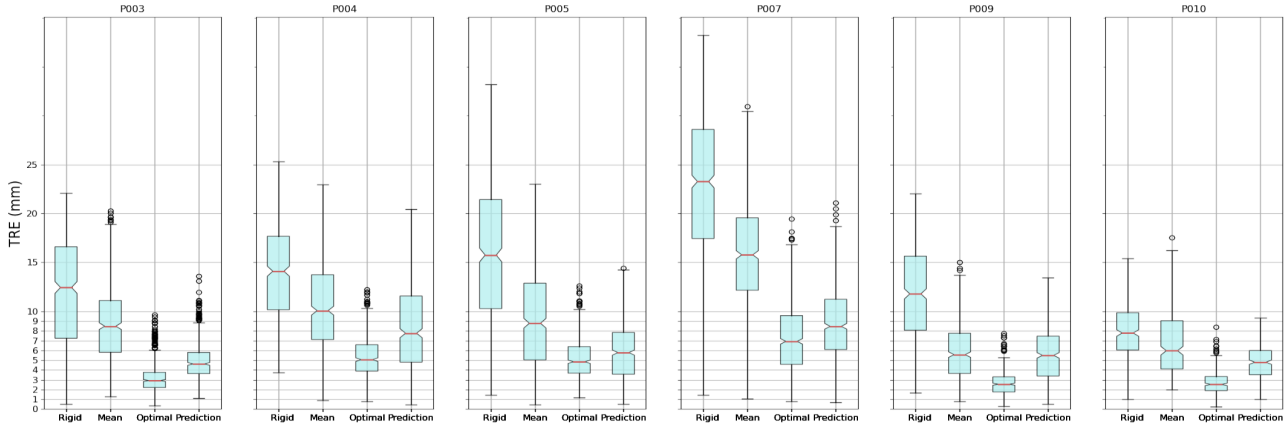

Figure 5. Prediction performance for the first 6 patients

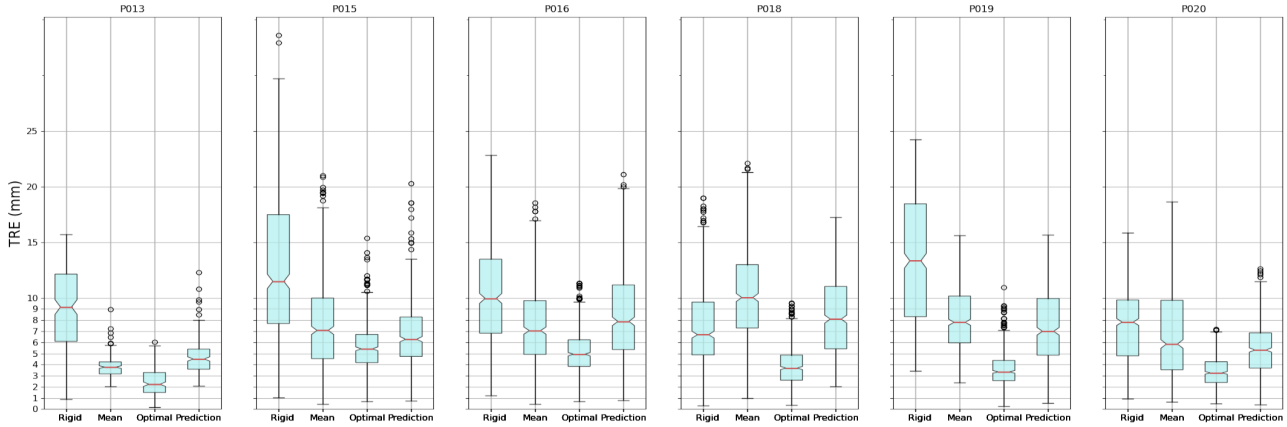

Figure 6. Prediction performance for the last 6 patients

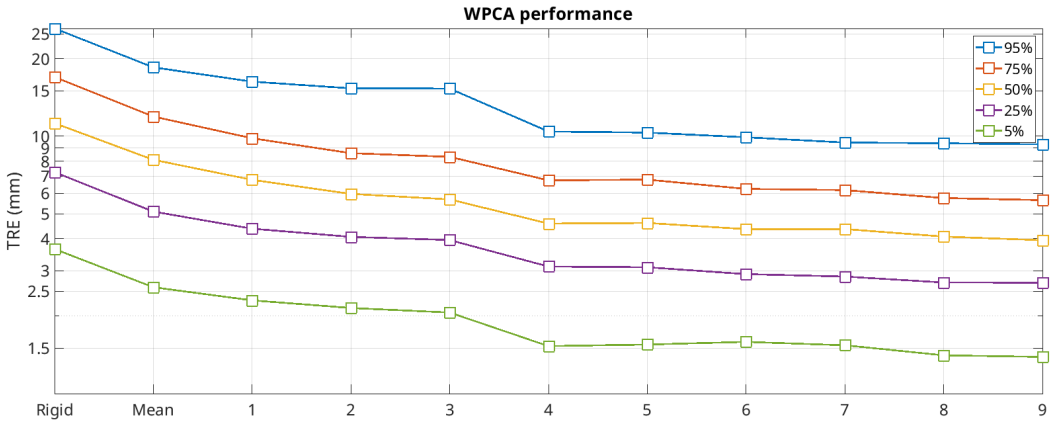

Figure 7. Performance of the wPCA data description as a function of the number of modes. The performance is measured by the impact of the number of modes on the distribution of errors (median value, quartiles and min and max limits) between the deformations modeled by the WPCA and the estimated deformations (reference truth).

4. DISCUSSION AND CONCLUSION

This paper presents a method for predicting lung deformations resulting from the change in the patient pose between preoperative and intraoperative configurations during a VATS procedure. The problem was approached as an inverse problem with the direct problem being a deformation model inferred from pose change deformations estimated on an intermediate imaging applied to a set of patients.

The accuracy of the deformation prediction was evaluated against its estimation using a leave one out cross validation (LOOCV). A simple rigid registration results in a average TRE median of 12.14 mm. This error is reduced to 8.09 mm by fitting an average model to the patient's data and to 6.33 mm by estimating the correct mode by solving the inverse problem.

These results were obtained with relatively few patients. However, our experiments show that we have some generalization in that, according to Fig. 7, we are able to significantly compensate for distortions on the test data with only 4 modes.

Our initial assumption is that the pleuropulmonary space did not undergo deformation between the change of pose (CBCT_1) and the pneumothorax (CBCT_2). In this case, the mode estimation is accurate and the cost function is convex. The direct model thus seems to pose the problem well, by capturing the link between the deformation of the lung surface and its internal deformation (*cf.* the results obtained by the (*Optimal*) mode). However, this hypothesis is not verified in reality. Pneumothorax often results in a collapse of the mediastinum and an upward movement of the diaphragm. Secondly, the costal pleura also undergoes a slight deformation during pneumothorax. This, combined with the problem of the limited field of view of CBCT_2, leads to results that are somewhat less accurate than expected (*cf.* the results obtained by the (*Prediction*) mode).

One solution that has been explored to solve these problems has been to incorporate into our model the deformations of the pleuropulmonary space associated with pneumothorax, however these deformations are not regular and in some cases may even degrade the performance of the PCA model. The success of a good solution of the inverse problem relies on the choice of the useful region points. Our experiments have shown that among the 4000 points of the lung surface initially present in the field of view of the CBCT_2, about 2500 are useful and lead to an accurate estimation. The problem now is to find the right heuristics to automatically identify the relevant regions.

Future work will consist of improving the inverse problem solving scheme. Moreover, we plan to evaluate the prediction of the deformations of the patient's position change on the complete framework,[2] *i.e.* on its capacity to initialize well the biomechanical model in order to predict the position of the nodule.

ACKNOWLEDGMENTS

The work presented in this article was supported by the Région Bretagne through its *Allocations de Recherche Doctorale* (ARED) framework and by the French National Research Agency (ANR) as part of the VATSop project (ANR-20-CE19-0015).

REFERENCES

[1] Rouzé, S., de Latour, B., Flécher, E., Guihaire, J., Castro, M., Corre, R., Haigron, P., and Verhoye, J.-P., "Small pulmonary nodule localization with cone beam computed tomography during video-assisted thoracic surgery: a feasibility study," *Interactive CardioVascular and Thoracic Surgery* **22**(6), 705–711 (2016).

[2] Alvarez, P., Rouzé, S., Miga, M. I., Payan, Y., Dillenseger, J.-L., and Chabanas, M., "A hybrid, image-based and biomechanics-based registration approach to markerless intraoperative nodule localization during video-assisted thoracoscopic surgery," *Medical Image Analysis* **69**, 101983 (2021).

[3] San Jose Estepar, R., Ross, J. C., Harmouche, R., Onieva, J., Diaz, A. A., and Washko, G. R., "Chest imaging platform: an open-source library and workstation for quantitative chest imaging," in [*American Thoracic Society 2015 International Conference*], *American Thoracic Society International Conference Abstracts*, A4975–A4975 (2015).

[4] Marstal, K., Berendsen, F., Staring, M., and Klein, S., "SimpleElastix: a user-friendly, multi-lingual library for medical image registration," in [*2016 IEEE Conference on Computer Vision and Pattern Recognition Workshops (CVPRW)*], IEEE (2016).

[5] Haber, E. and Modersitzki, J., "Intensity Gradient Based Registration and Fusion of Multi-modal Images," in [*Medical Image Computing and Computer-Assisted Intervention – MICCAI 2006*], Larsen, R., Nielsen, M., and Sporring, J., eds., *Lecture Notes in Computer Science*, 726–733, Springer (2006).

[6] Wu, Z. Y., Rietzel, E., Boldea, V., Sarrut, D., and Sharp, G., "Evaluation of deformable registration of patient lung 4DCT with sub-anatomical region segmentations," *Medical Physics* **35**(2), 775 (2008).

[7] Danielsson, P.-E., "Euclidean distance mapping," *Computer Graphics and Image Processing* **14**(3), 227–248 (1980).

[8] Bailey, S., "Principal component analysis with noisy and/or missing data," *Publications of the Astronomical Society of the Pacific* **124**(919), 1015–1023 (2012).